Mn-dopant-induced effects in $Zn_{1-x}Mn_xO$ compounds

2007 J. Phys.: Condens. Matter 19 476214

(http://iopscience.iop.org/0953-8984/19/47/476214)

IOP PUBLISHING JOURNAL OF PHYSICS: CONDENSED MATTER

J. Phys.: Condens. Matter **19** (2007) 476214 (8pp) doi:10.1088/0953-8984/19/47/476214

Mn-dopant-induced effects in $Zn_{1-x}Mn_xO$ compounds

S Riyadi[1], Muafif[1], A A Nugroho[1], A Rusydi[1,2] and M O Tjia[1]

[1] Faculty of Mathematics and Natural Sciences, Institut Teknologi Bandung, Jalan Ganesha 10, 40132 Bandung, Indonesia
[2] Institut für Angewandte Physik, Universitat Hamburg, Jungiusstraße 11, D-20355 Hamburg, Germany

E-mail: nugroho@fi.itb.ac.id

Received 2 July 2007, in final form 11 October 2007
Published 1 November 2007
Online at stacks.iop.org/JPhysCM/19/476214

Abstract

An experimental study on Mn-dopant-induced effects in $Zn_{1-x}Mn_xO$ was performed for samples with $x = 0.02$, 0.04, 0.06, and 0.08, which were prepared by solid state reaction at 1200 °C. The result of x-ray diffraction refinement analysis did not turn up evidence of Mn_xO_y cluster inclusion over the entire doping range, while the structural parameter variations indicate a solubility limit of about 6% for Mn^{2+} and incorporation of Mn ions of higher valency at higher dopant levels. The magnetization data exhibit mostly intrinsic antiferromagnetic instead of ferromagnetic properties, as predicted by more recent theoretical works. The substitutional incorporation of the Mn in ZnO was further confirmed by the associated broad-band photoluminescence spectra. The suggested incorporation of Mn ions of higher valency at higher dopant concentration was also supported by the related x-ray photoemission data, and in agreement with a previous theoretical prediction.

(Some figures in this article are in colour only in the electronic version)

1. Introduction

The potential occurrence of room-temperature ferromagnetism (RTF) in Mn-doped ZnO as predicted theoretically by Dietl *et al* [1] has attracted intense research interest, as the host material is a well known highly stable wide-gap semiconductor which is readily available at relatively inexpensive price. If the prediction were right, it could be applied with high technological impact as a very useful transparent diluted magnetic semiconductor (DMS) for spintronic and magneto-optical devices. This explains the large number of subsequent experimental works carried out to try and verify or clarify the theoretical prediction. Unfortunately, in contrast to the more or less established experimental confirmation of high-temperature ferromagnetism in Mn-doped GaN [2–5], the reports on Mn-doped ZnO have so far been controversial, as described below.

Sharma *et al* were the first to report the experimental indication of ferromagnetism both in bulk and pulsed laser deposited (PLD) thin films of Mn-doped ZnO [6, 7]. They reported the occurrence of ferromagnetism in Mn-doped ZnO above room temperature without the need for additional hole carriers. However, their works posed serious question about the origin of the ferromagnetic contribution since their samples were not shown to be free from manganese oxide inclusions. Other groups also reported the ferromagnetic properties of ZnO-based DMS [8, 9], although they did not show the associated Curie–Weiss behavior (M–T curve). Still another series of experimental works showed, on the other hand, that Mn-doped ZnO did not even exhibit the predicted ferromagnetic phase; the samples displayed instead either paramagnetic or antiferromagnetic properties [10–13]. Meanwhile, Blythe *et al* claimed to have observed ferromagnetic evidence from Mn-doped ZnO samples by greatly prolonging the grinding process in the synthesis of the bulk samples by solid state reaction [14]. Again, the possibility of contribution from the magnetic impurity phase was not explicitly addressed. Chen *et al* further showed that Mn-doped ZnO bulk samples sintered in air did not exhibit the much-coveted ferromagnetic behavior [15].

It is interesting to note in this connection that in some recent reports on the theoretical front, relatively consistent results are emerging with a clear message pointing to the need for different doping schemes for the realization of previous theoretical predictions concerning Mn-doped ZnO. To be specific, one may cite the theoretical work of Spaldin [16] employing the local spin density approximation (LSDA) and special pseudopotential model, which suggested the need for additional p-doping beside Mn in order to produce robust ferromagnetism in ZnO-based DMS. A subsequent LSDA-based theoretical analysis by Sluiter *et al* [17] showed the crucial role of the defect-induced state which was verified in their experimental demonstration of room-temperature ferromagnetism in $Zn_{1-x-y}Li_xCo_yO$. In a more recent report, Petit *et al* [18] showed that by introducing self-interaction (SI) into the LSDA scheme, they were able to show specifically that the presence of additional nitrogen (p-type) dopant in excess of the transition metal dopant was needed to delocalize the d-states responsible for the carrier-mediated double exchange ferromagnetic interaction. This was further supported by the work of Kittilstvedt *et al* [19] on dopant polarity-dependent ferromagnetism on the basis of electronic structure data for Mn-doped samples. It was revealed that additional p-type dopant was needed to promote the dopant–defect hybridization responsible for the high-temperature ferromagnetism.

Meanwhile, reports on the experimental indication of ferromagnetic properties of the (Zn, Mn)O system continued to appear both in the form of thin films and bulk samples. In the case of magnetron sputtering deposited thin film [20], only a hysteretic M–H curve measured at 5 K was explicitly displayed, although a T_c of around 62 K was inferred from the M–T curve. For the atomic layer deposited film [21], a weak ferromagnetism was inferred from ESR spectra at $T = 296$ K, while from pulsed laser deposited film [22], a room-temperature ferromagnetic hysteresis loop was demonstrated. In the case of bulk sample synthesized by solid state reaction [23], the M–H data did not indicate the appearance of robust hysteretic ferromagnetic behavior. In the light of these inconclusive results, additional structural information about the compound in combination with magnetic data and results of other complementary measurements should still be useful for further clarification of the persisting controversies.

The purpose of this work was to verify some of the aforementioned theoretical results by investigating the presence of intrinsic ferromagnetism in the purely Mn-doped ZnO in the absence of impurity inclusion. The substitutional incorporation of Mn in the compound is to be further examined and confirmed by detailed structural characterization together with measurements of other related dopant-induced physical effects. For this propose, the Mn-doped ZnO ($Zn_{1-x}Mn_xO$) polycrystalline samples prepared with various x were subject to

detailed structural analysis on the basis of XRD data. In addition to examining the presence of impurity clusters, the structural variations with respect to increasing Mn-dopant concentration were examined in relation to the possible variation of the Mn oxidation state. The magnetization measurement was then performed to investigate the intrinsic magnetic properties of those samples. Additional measurements of photoluminescence (PL) and x-ray photoemission spectroscopy (XPS) spectra were carried out to investigate the associated dopant-induced changes in the optical properties of the samples and the related changes of their electronic structure.

2. Experiments

The polycrystalline samples of $Zn_{1-x}Mn_xO$ were synthesized by the standard solid state reaction method with $x = 0.02$, 0.04, 0.06, and 0.08. The starting materials were mixtures of ZnO (99.999%) and MnO powders. The MnO powder was obtained from the reduction of MnO_2 powder (99.99%) in a H_2 environment at 900 °C. All of the chemicals were dried in the furnace at 150 °C before being mixed as the starting materials with various Mn concentrations as stated above. The mixtures were subsequently ball milled and pressed into pellets for the sintering process at 1200 °C for 5 h.

The structural analysis was performed on data obtained by repeated step-wise x-ray diffraction measurements over a long data acquisition time (nearly 10 h) using a Bruker D8 diffractometer in the range of 2θ between 20° and 100°. Refinement of those data for elucidating the lattice parameters and atomic positions was conducted with GSAS software by fitting the powder diffraction patterns with that deduced from the appropriate structural model. The temperature dependence of magnetization curve were measured by means of a SQUID magnetometer (Quantum Design MPMS-7). The measurement was carried out in a 1000 Oe magnetic field in zero-field cooled (ZFC) mode. The effective magnetic moments (μ_{eff}) as well as the Curie–Weiss constants were extracted from the temperature dependence of inverse magnetic susceptibilities.

Additionally, the substitutional effect of the dopants was further examined by PL spectroscopy for the indication of the expected dopant-induced variation of optical properties. This was further compared with the possible changes in electronic properties (e.g. oxidation states) of Mn in ZnO using XPS data.

3. Results and discussion

Figure 1 shows the observed XRD patterns along with their fitted patterns. The structural analysis was first performed by fitting the measured XRD pattern with those derived from the structural model of ZnO which has a wurtzite hexagonal crystal structure with space group $P6_3mc$ by means of the GSAS program. Each atom in this structure has a multiplicity of 2 and resides on the 2b Wyckoff position with $z = 0$ for the Zn atom and $z = 5/8$ for the O atom. The 'impurity' peaks at 2θ around 29° and 33° found in Mn-doped samples are also observed in the undoped sample. These 'impurity' peaks are therefore excluded in the analysis. The differences between the observed and fitted patterns are indicated in terms of discrepancy factors (χ^2, R_{wp}, R_p) at the bottom of table 1, which measure the credibility of our result. Based on this analysis, no meaningful indication of the presence of the Mn_xO_y impurity phase was found in agreement with a previous report [13], and in contrast to the frequently made statement about the likelihood of Mn_xO_y cluster formation at high sintering temperature [6].

Figure 2 shows the changes in lattice parameters with increasing Mn concentration. The shifted scale positions adopted for the a and c parameter variations are intended for easy

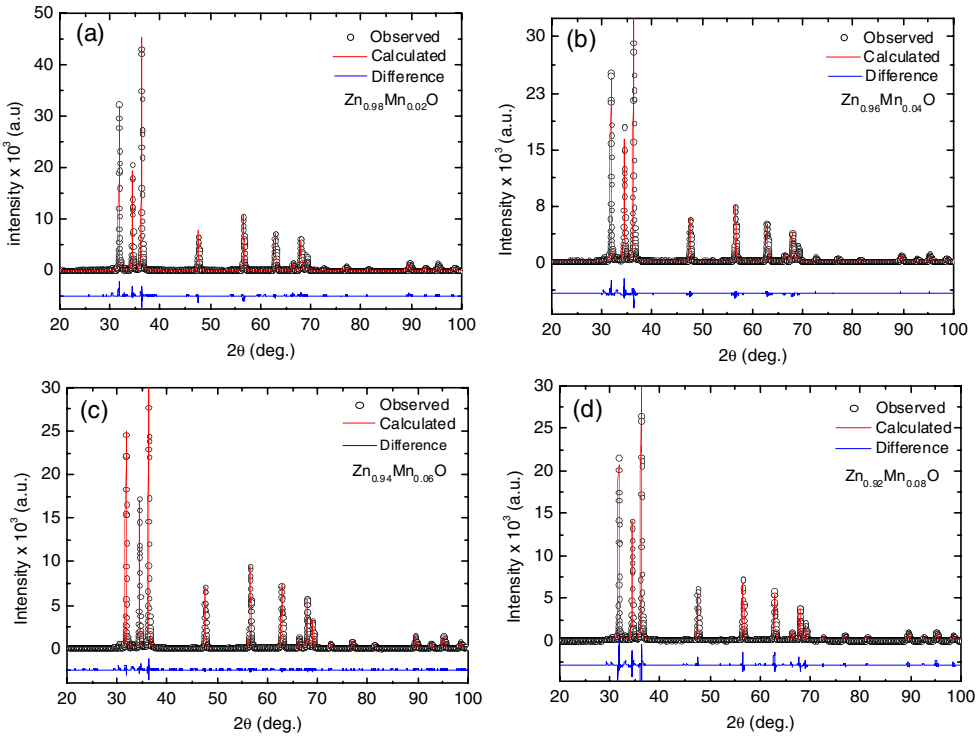

Figure 1. The observed, refined, and corresponding difference XRD patterns for $Zn_{1-x}Mn_xO$ samples sintered at 1200 °C for samples with (a) $x = 0.02$, (b) $x = 0.04$, (c) $x = 0.06$, and (d) $x = 0.08$.

Table 1. Refinement parameters for samples sintered at 1200 °C.

		2% Mn	4% Mn	6% Mn	8% Mn
a (Å)		3.251 415	3.253 253	3.256 409	3.255 627
c (Å)		5.207 802	5.209 900	5.212 968	5.211 053
V (Å^3)		47.679	47.752	47.873	47.833
Atoms					
Zn	z	−0.015 800	0.000 394	−0.003 295	0.077 265
O	z	0.607 625	0.636 040	0.617 186	0.687 510
Mn	z	−0.015 800	0.000 394	−0.003 295	0.077 265
Discrepancy factors					
χ^2		3.78	3.34	3.60	3.75
R_p (%)		5.60	5.38	5.16	5.69
R_{wp} (%)		8.30	8.08	8.67	9.31

comparison. As noted in the graph, there is a closely similar monotonic increase of both lattice parameters up to 6% of Mn (with a total increase of the order of 0.01 Å), in agreement with the growing substitution of Mn^{2+} which, in a tetrahedral coordination, has a larger ionic radius (0.66 Å) compared to that of Zn^{2+} in the same coordination (0.60 Å) [20]. Beyond that, the lattice parameters begin to decrease. In view of the absence of Mn_xO_y impurity, this information may be taken as a clue to the further substitutional incorporation of Mn ions in the

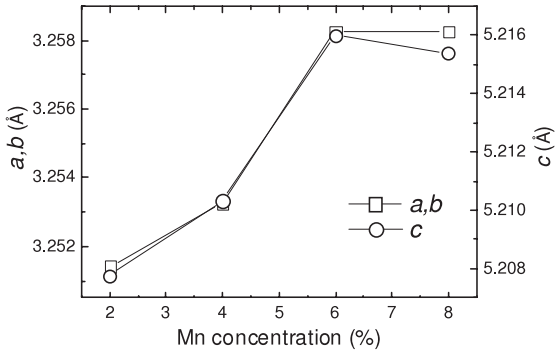

Figure 2. Changes in a, b, and c lattice parameters as functions of Mn content. Note that the scale positions for a and c are shifted relative to each other.

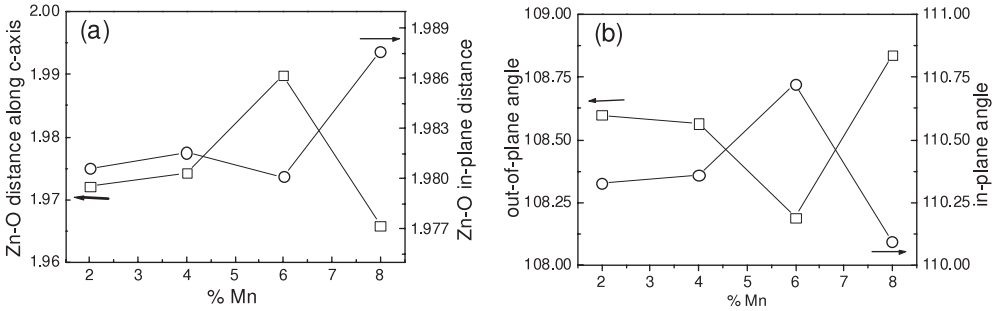

Figure 3. Variations of (a) the out-of-plane ($\|c$) and in-plane ($\perp c$) Zn–O bond length and (b) the out-of-plane and in-plane O–Zn–O bond angle for samples synthesized at 1200 °C.

valence state of either Mn^{3+} or Mn^{4+}; both are known to have smaller ionic radii than that of Mn^{2+}. In other words, the 6% dopant concentration can be regarded roughly as an estimate of solid solubility of Mn^{2+} in ZnO, which is considerably lower than the figures reported for a thin film sample [24, 25].

Figure 3 shows the changes in the Zn–O bond lengths (a) and O–Zn–O bond angles (b), each deduced from data in figure 2 as a function of Mn concentration. It is seen that the increase in Zn–O bond length along the c-axis up to 6% of Mn is accompanied by the shrinkage of the in-plane Zn–O bond length. Both of these trends are reversed when the Mn concentration exceeds 6%. A similar trend of variations is exhibited by the Zn–O–Zn bond angle. In all cases, non-monotonic variations feature strongly, with turning points occurring around a Mn concentration of 6%. While this general pattern shares some basic characteristics with the non-monotonic behavior shown in figure 2, the opposite trends of variations displayed by the different atomic bond lengths and bond angles defy simple correlational interpretation. It appears that these changes of atomic coordinates somehow conspire to produce the observed variation pattern of lattice parameters shown in figure 2.

Figure 4(a) shows the plots of magnetization curves as functions of temperature for $Zn_{1-x}Mn_xO$ with nominal x of 0.02, 0.04, and 0.08. The Curie–Weiss constants were extracted from the curves of inverse susceptibility versus temperature as illustrated in figure 4(b). The resulting Curie–Weiss temperature of $T_{cw} = 10.88$ K for $x = 0.02$ indicates ferromagnetic interaction, while the obtained values of $T_{cw} = -36.97$ K for $x = 0.04$ and $T_{cw} = -63.89$ K for $x = 0.08$ clearly signify antiferromagnetic interaction. The associated effective moments per Mn ion determined from the data were found to yield values of 0.10, 0.29, and 0.13 μ_B, respectively, for those samples. It is to be noted that the samples at higher dopant concentrations

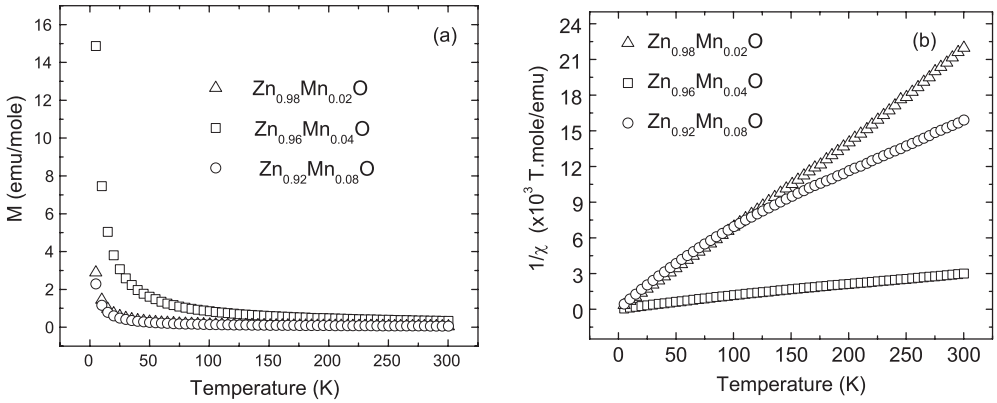

Figure 4. (a) Plots of magnetization as functions of temperature for $Zn_{1-x}Mn_xO$ with nominal x of 0.02, 0.04, and 0.08. (b) Corresponding temperature dependence of the inverse susceptibility.

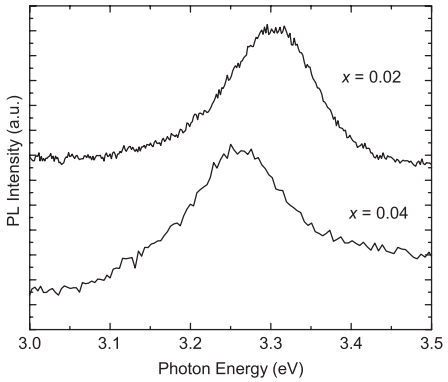

Figure 5. The photoluminescence spectra of $Zn_{1-x}Mn_xO$ with $x = 0.02$ and 0.04.

generally show unambiguous antiferromagnetic properties as reported previously [13]. The exception found for $x = 0.02$ is at best a faint, and hence inconclusive, ferromagnetic signal marked by a very small Curie–Weiss constant. The appearance of a growing antiferromagnetic response at higher dopant concentrations is nevertheless an issue that has yet to be more thoroughly addressed.

As reported previously [26], the substitutional incorporation of Mn in ZnO led to certain changes in the PL spectrum of the compound. In order to lend support to our earlier suggestion on Mn incorporation in ZnO from the XRD data analysis, photoluminescence spectra were measured for $Zn_{1-x}Mn_xO$ with $x = 0.02$ and 0.04. The so-called broad-band emission spectra of the doped samples obtained by photo-excitation with 305 nm monochromatic radiation are shown in figure 5. As seen in the figure, the peaks of both spectra are downshifted below the gap energy of ZnO (3.37 eV) to 3.29 eV and 3.26 eV for $x = 0.02$ and 0.04, respectively. We also note that, the addition of Mn in ZnO results in further downshift of the peak (negative energy shift) in conjunction with a slight broadening of the spectrum. These features are basically similar to those reported previously for Mn-doped ZnO thin film [26, 27], although the dopant-induced quenching effect is not perceptible here due to the much lower dopant concentrations investigated in our bulk samples. This result signifies the appearance of growing impurity-induced gap states and thereby confirms the substitutional incorporation of Mn ions in the crystals.

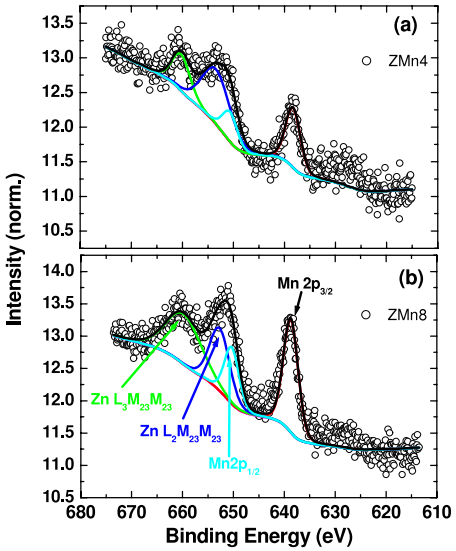

Figure 6. The fit of XPS spectra for $Zn_{1-x}Mn_xO$ with (a) $x = 0.04$ and (b) $x = 0.08$.

It has been widely held that the Mn-dopant in the (Zn, Mn)O compound has a valence state of 2+, although a recent LSDA calculation [17] suggested that Mn^{3+} is more favored in the system's ground state. In a more recent study [19], a resonance between Mn^{2+} and Mn^{3+} was proposed involving a charge transfer process between the dopant and the ligand (or the semiconductor lattice) conduction band. This issue is examined in this work by performing the XPS measurement on the samples with an Al Kα ray source ($h\nu = 1486.6$ eV) and an energy resolution of 1 eV. For the purpose of the ensuing discussion, we focused on the measurement of Mn peaks using XPS at a binding energy of around 600 eV. To overcome the relatively weak signal due to the low concentration of Mn-dopant, especially on the sample surface, the S/N ratio was enhanced by taking the averaged results of 25 measurements for each sample. After being processed by removing the satellite peaks and ghost lines in the data, the data were fitted with a sum of Gaussian and Lorentzian line shapes in a ratio of about 80%. The resulted spectra along with the fitted curves and the related Auger lines are presented in figures 6(a) and (b) for the samples with 4% and 8% Mn-dopant, respectively. The manganese $2p_{1/2}$ and $2p_{3/2}$ orbitals in 2+ oxidation states of MnO are clearly exhibited at around 650 and 639 eV, respectively. One notes further that the peaks for case (b) are both higher and sharper, in agreement with the more dominant presence of the Mn-dopant. Interestingly, the Auger spectral distribution of Zn $L_{2,3}M_{23}M_{23}$ increases with increasing Mn-dopant. It is known that those transitions are directly related to an effective Coulomb interaction U_{eff} between two 3d holes of Zn on the same site. Therefore, this may imply that the oxidation state of the dopant is higher than 2+ and that is strongly hybridized with Zn. The excess charges increase the Auger spectral distributions for the sample with 8% dopant. The slight energy up-shifts (barely visible in the figure but clearly indicated in the data, e.g. $\Delta E = 0.6$ eV for the $2p_{3/2}$ peak) may further support the presence of an oxidation state higher than 2+, corresponding to smaller ionic radius. It must be admitted, however, that this point requires further verification.

4. Conclusion

We have presented in this report the results of refinement analysis of the x-ray diffraction data obtained from samples of $Zn_{1-x}Mn_xO$ in the form of bulk polycrystallines with various dopant

concentrations. The refinement result indicates the absence of Mn_xO_y clusters for x up to 0.08. The variations of lattice parameter revealed by the analysis also imply the effective substitution of Zn by Mn for the doping range considered, with possible change in the oxidation state of incorporated Mn at $x > 6\%$. This suggested substitutional incorporation of Mn in ZnO was confirmed by the result of PL measurement. The magnetization data obtained from these impurity-free samples indicate mostly antiferromagnetic interaction, which is in agreement with most recent theoretical analysis. Further XPS data obtained from the samples are also consistent with the suggested incorporation of Mn ions of higher valance state at higher dopant concentration, as predicted theoretically.

Acknowledgments

This work was supported by a research grant from the Directorate General of Higher Education with contract no. 13b/K.01.7.6/PHKB/2005. We also thank Thom Palstra for the useful discussions and the chance to perform the measurements at the Zernike Institute for Advanced Materials, Rijksuniversiteit Groningen. We also would like to thank DELTA for providing Syarif Riyadi with living costs during his 3 months of research at the Zernike Institute for Advanced Materials.

References

[1] Dietl T, Ohno H, Matsukura F, Cibert J and Ferrand D 2000 *Science* **287** 1019
[2] Reed M L, El-Masry N A, Stadelmaier H H, Ritums M K, Reed M J, Parker C A, Roberts J C and Bedair S M 2000 *Appl. Phys. Lett.* **79** 3473
[3] Linnarsson M, Janzén E, Monemar B, Kleverman M and Thilderkvist A 1997 *Phys. Rev.* B **55** 6938
[4] Overberg M E, Abernathy C R, Pearton S J, Theodoropoulou N A, McCarthy K T and Hebard A F 2001 *Appl. Phys. Lett.* **79** 1312
[5] Jung S W, An S-J, Yi G-C, Jung C U, Lee S-I and Cho S 2002 *Appl. Phys. Lett.* **80** 4561
[6] Sharma P, Gupta A, Rao K V, Owens F J, Sharma R, Ahuja R, Osorio Guillen J M, Johansson B and Gehring G A 2003 *Nat. Mater.* **2** 673
[7] Sharma P, Gupta A, Owens F J, Inoue A and Rao K V 2004 *J. Magn. Magn. Mater.* **282** 115
[8] Kolesnik S, Dabrowski B and Mais J 2004 *J. Appl. Phys.* **95** 2582
[9] Venkatesan M, Fitzgerald C B, Lunney J G and Coey J M D 2004 *Phys. Rev. Lett.* **93** 177206
[10] Roy V A L, Djurišić A B, Liu H, Zhang X X, Leung Y H, Xie M H, Gao J, Lui H F and Surya C 2004 *Appl. Phys. Lett.* **84** 756
[11] Cheng X M and Chien C L 2003 *J. Appl. Phys.* **93** 7876
[12] Yoon S W, Cho S-B, We S C, Yoon S, Suh B J, Song H K and Shin Y J 2003 *J. Appl. Phys.* **93** 7879
[13] Lawes G, Risbud A S, Ramirez A P and Seshadri R 2005 *Phys. Rev.* B **71** 045201
[14] Blythe H J, Ibrahim R M, Gehring R A, Neal J R and Fox A M 2004 *J. Magn. Magn. Mater.* **283** 117
[15] Chen W, Zhao L F, Wang Y Q, Miao J H, Liu S, Xia Z C and Yuan S L 2005 *Solid State Commun.* **134** 827
[16] Spaldin N A 2004 *Phys. Rev.* B **69** 125201
[17] Sluiter M H F, Kawazoe Y, Sharma P, Inoue A, Raju A R, Rout C and Waghmare U V 2005 *Phys. Rev. Lett.* **94** 187204
[18] Petit L, Schulthess T C, Svane A, Szotek Z, Temmerman W M and Janotti A 2006 *Phys. Rev.* B **73** 045107
[19] Kittilstvedt K R, Liu W K and Gamelin D R 2006 *Nat. Mater.* **5** 291
[20] Xu H Y, Liu Y C, Xu C S, Liu Y X, Lhao C L and Mu R 2006 *J. Chem. Phys.* **124** 074707
[21] Lasley-Hunter B, Hunter B, Noginov M, Dadson J B, Zhang K, Rakhimov R R, Pradhan A K, Zhang J and Sellmyer D J 2006 *J. Appl. Phys.* **99** 08M116
[22] Wójcik A, Kopalko K, Godlewski M, Guziewicz E, Jakiela R, Minikayev M and Paszkowicz W 2006 *Appl. Phys. Lett.* **89** 051907
[23] Jayakumar O D, Gopalakrishnan I K and Kulshrestha S K 2006 *Physica* B **381** 194
[24] Fukumura T, Jin Z, Ohtomo A, Koinuma H and Kawasaki M 1999 *Appl. Phys. Lett.* **75** 3366
[25] Fukumura T, Jin Z, Kawasaki M, Hasegawa T, Koshihara T and Koinuma H 2001 *Appl. Phys. Lett.* **78** 958
[26] Nakayama M, Tanaka H, Masuko K, Fukushima T, Ahida A and Fujimura N *Appl. Phys. Lett.* **88** 241908
[27] Zheng-Wu J, Yoo Y Z, Sekiguchi T, Chikyow T, Ofuchi H, Fujoka H, Oshima M and Koinuma H 2001 *Appl. Phys. Lett.* **78** 3824